

Nonlinearity of the unsteady aerodynamics of the viscous flow on supercritical wing in transonic regime

Kenichi Saitoh

Japan Aerospace Exploration Agency, Japan

Keywords: Limit Cycle Oscillation, Transonic, Unsteady aerodynamics

Abstract. Unsteady aerodynamics of two dimensional supercritical wing profile in transonic regime was investigated by Navier-Stokes code. First harmonic components of the unsteady aerodynamics obtained by simulation for forced oscillations of heaving and pitching mode were plotted to the amplitude of oscillations and it shows nonlinearity of the unsteady aerodynamics in small amplitude region. Stability analysis based on the first harmonic components of the unsteady aerodynamics also shows nonlinear trend. Limit Cycle Oscillation (LCO) of small amplitude about 0.1 deg. could exist from the stability analysis and simulation was carried out. Nonlinearity of unsteady aerodynamics in small amplitude range is affected by transition point, which interferes with unsteady pressure distribution in local supersonic region on upper surface. These computational results are described in this paper.

1 INTRODUCTION

Schewe et al. found small amplitude LCO which has about 0.2 deg. of pitching oscillation in transonic wind tunnel test with two dimensional elastic support system^[1]. This implies it has nonlinearity in small amplitude region, but the LCO is thought different from a typical one which is induced by the shock wave motion on the wing surface and limited the amplitude by the flow separation. Castro showed to simulate small amplitude LCO by considering perforated wind tunnel wall effect in his CFD analysis^[2]. Thomas showed a relation between amplitude of the pitching oscillation of the LCO and flutter speed using Harmonic Balance method^[3], but no small amplitude LCO was shown.

Characteristics of the transonic unsteady aerodynamics especially in small amplitude oscillation are investigated by the CFD analysis for NLR-7301 supercritical wing profile in this paper.

2 ANALYSIS METHOD

2.1 Equation of binary aeroelastic system

Schematic binary aeroelastic system is shown in Figure 1, and equation of the system is as follows.

$$\begin{bmatrix} 1 & x_a \\ x_a & r_a^2 \end{bmatrix} \begin{bmatrix} \ddot{h}^* \\ \ddot{\alpha}^* \end{bmatrix} + \begin{bmatrix} 2\zeta_h \omega_h^* & 0 \\ 0 & r_a^2 2\zeta_\alpha \omega_\alpha^* \end{bmatrix} \begin{bmatrix} \dot{h}^* \\ \dot{\alpha}^* \end{bmatrix} + \begin{bmatrix} \omega_h^{*2} & 0 \\ 0 & r_a^2 \omega_\alpha^{*2} \end{bmatrix} \begin{bmatrix} h \\ \alpha \end{bmatrix} = \frac{1}{\mu\pi} \begin{bmatrix} -C_l \\ 2C_m \end{bmatrix} \quad (1)$$

The equation is nondimensionalized by half chord length b for length, total mass m for mass and b/U for time, where U is uniform speed of flow. Asterisk means values based on non-dimensional time. Structural parameters of reference [1] are converted for Eq. (1) and listed in table 1. Eq. (1) is also expressed as Eq. (2) in this paper.

$$M\ddot{q} + C\dot{q} + Kq = f \quad (2)$$

2.2 Numerical analysis

Navier-Stokes code used for the analysis is based on the thin layer NS equation and Baldwin-Lomax turbulence model is adopted^[4]. Structural mode equation combined with the aerodynamics is integrated by Wilson’s implicit θ method. Structured C type grid of which size is 313x79 is generated and 247 grid points are placed on the wing surface. Thickness of the grid on the wing is $6 \times 10^{-5}b$ and far field boundary is $40b$. Time step size for unsteady analyses is about 0.002 in non-dimensional time. Courant number is about 30. In LCO simulations, 0.001 is taken as time step size to converge results.

Wing profile data of reference [5] is used. The trailing edge of the data is at $x/c=1.015$, but in this analysis the profile is cut at $x/c =1.0$ to combine upper and lower surface at the center in thickness. So the line between leading and trailing edge has -0.16 deg inclination.

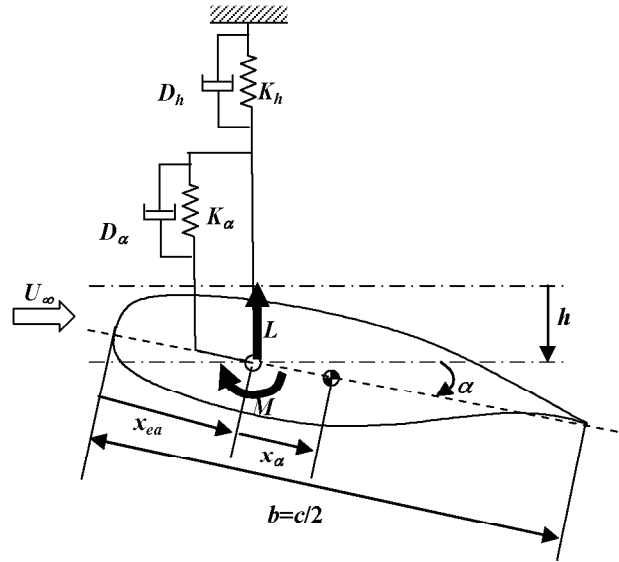


Figure 1 : Two dimensional aeroelastic system

Table 1 : Structural parameters

reference length (half chord length)	b	$= 0.15 \text{ [m]}$
center of rotation	x_{ea}	$= 0.50$
static unbalance	x_α	$= 0.0968$
radius of gyration	r_α	$= 0.394$
pitching frequency	ω_α^*	$= 0.1584 = \sqrt{K_\alpha / I_\alpha} b / U_\infty$
heaving frequency	ω_h^*	$= 0.1204 = \sqrt{K_h / mb} / U_\infty$
damping of pitching	ζ_α	$= 0.0043 = D_\alpha / (2\sqrt{K_\alpha I_\alpha})$
damping of heaving	ζ_h	$= 0.0071 = D_h / (2\sqrt{K_h m})$

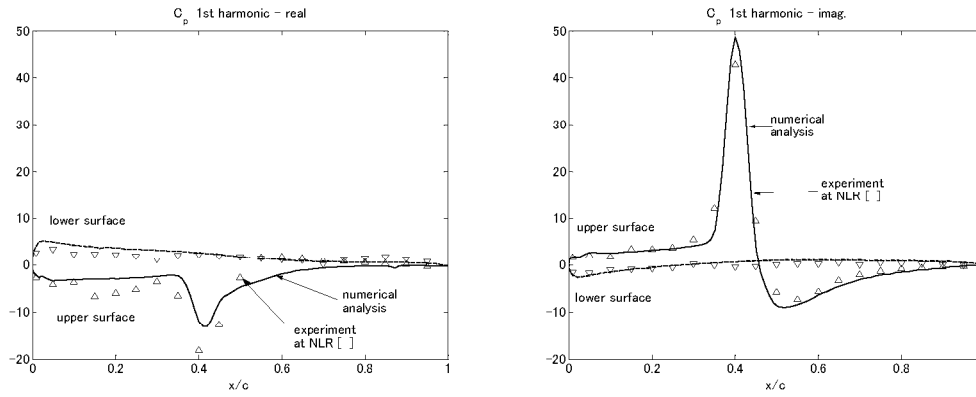


Figure 2 : Comparison of CFD with experiment; case CT-5^[5]

The code is validated by comparing to the AGARD test case^{[5][6]} of the same wing profile. The experimental data of which Mach number is 0.70 and mean angle of attack is 2.0 deg. has well developed shock. The numerical result shows reasonable results compared with the data (Figure 2).

2.3 Fourier series expansion of unsteady aerodynamics

To evaluate unsteady aerodynamics and analyze the stability of the aeroelastic system, numerical simulation was performed for 5 periods with heaving and/or pitching forced oscillation and Fourier coefficients were obtained from time histories of the aerodynamics. When a forced oscillation mode is

$q = (q_{1,r} + iq_{1,i})e^{i\omega t}$, first harmonic component of generated unsteady aerodynamics is

$f_1 = (f_{1,r} + if_{1,i})e^{i\omega t}$, where $f_{1,r}$ and $f_{1,i}$ are in and out of phase with the oscillation. Unsteady

aerodynamics including 0th and higher order is expressed as followings.

$$f = f_0 + \sum_{m=1}^{\infty} (f_{m,r} + if_{m,i})e^{im\omega t} \quad (3)$$

Effect of harmonic components of unsteady aerodynamics on the system stability is considered here.

When the system is in harmonic oscillation, the energy of the system given by the flow is

$$\oint_{S_H} f^T \frac{dq}{dt} dt \quad (4)$$

where f is unsteady aerodynamics and S_H is trajectory of the system. According to the Eq.(1) the energy given by flow in one period is

$$\frac{1}{\mu\pi} \int_0^{2\pi/\omega^*} (-C_l \dot{h}^* + 2C_m \dot{\alpha}^*) dt^* \quad (5)$$

Substituting the complex Fourier series expansion

$$q = q_0 + \sum_{l=1}^{\infty} (q_l e^{il\omega t} + \bar{q}_l e^{-il\omega t}), \quad f = f_0 + \sum_{m=1}^{\infty} (f_m e^{im\omega t} + \bar{f}_m e^{-im\omega t}) \quad (6)$$

into Eq. (4), it become 0 when $m \neq l$ because of orthogonality of Fourier series expansion. Where \bar{q} , \bar{f} are complex conjugate of q , f respectively. When the system oscillates on first harmonic trajectory, the energy of the system given by flow can be specified by the first harmonic components of the unsteady aerodynamics. Subtracting energy dissipation of structural damping from Eq. (4), we can tell whether the system in sinusoidal oscillation is getting energy or not.

When the trajectory of LCO is S_L , the system energy getting from the flow is

$$\oint_{S_L} f^T \frac{dq}{dt} - e_d \quad (7)$$

where e_d means energy dissipation by structural damping. The difference of energy flux between sinusoidal oscillation and LCO is higher order components of the trajectory of the LCO. This means, if the LCO trajectory is close to sinusoidal motion, the stability of the LCO can be specified by the first harmonic component of the aerodynamics.

Furthermore, superposing of unsteady aerodynamics is valid if its amplitude is infinitesimally small, otherwise it always has an error to the nonlinear system.

2.4 Stability analysis

The unsteady aerodynamics will be evaluated according to the amplitude of oscillation and the dependency of the system stability to the amplitude will be investigated. Unsteady aerodynamic coefficients such as C_l and C_m are calculated for various amplitude and reduced frequency of forced heaving and pitching oscillation mode. Superposing those C_l and C_m , stability analysis can be performed out by $p-k$ method. The experiment^[1] indicated reduced frequency at LCO was nearly 0.12, therefore unsteady aerodynamics are calculated for $k=0.10, 0.12$ and 0.15 . For the $p-k$ method, those are interpolated like linear manner. Although the amplitude ratio between heaving and pitching mode for the unsteady aerodynamics should be the same to that of the unstable mode vector, $\bar{h}/\alpha=1.32$ was used for all cases, which was evaluated by experiment and some analysis previously done.

To exclude the superposing effect of the unsteady aerodynamics, Newton-Raphson method^[3] solving Eq.(1) is used. Sinusoidal oscillation representing LCO can be expressed as $q_1 e^{i\omega t}$, where $q_1 = [h_r + ih_i \quad \alpha_1]^T$, based on the pitching oscillation. If unsteady aerodynamics is expressed as $f_1 e^{i\omega t}$, Eq. (2) become

$$\{\omega^2 M + i\omega C + K\} q_1 e^{i\omega t} = f_1 e^{i\omega t} \quad (8)$$

Unknown parameters $L = [\omega \quad \mu \quad h_r \quad h_i]^T$ can be solved based on

$$R = \{\omega^2 M + i\omega C + K\} q_1 - f_1 = 0 \quad (9)$$

By Newton-Raphson method, L can be solved iteratively as

$$L^{n+1} = L^n - \left(\frac{\partial R^n}{\partial L^n} \right)^{-1} R^n \quad (10)$$

$\partial R^n / \partial L^n$ can be solved analytically because it is explicit function of L . Iteration will be continued until difference between L^{n+1} and L^n become small enough, in this case relative error become 10^{-6} . Results of p - k analysis was taken as initial value of L . Reference [3] indicate linear solution could bring good convergence. Based on the converged value of $h_r + ih_i$ and ω , unsteady aerodynamics should be calculated again. In this paper, this iteration was done twice and difference of flutter index between before and after iteration 1% at maximum.

Although mean value of α should be taken into account because it has important role for unsteady aerodynamics, in this paper it is fixed for the analysis to avoid complexity.

3. RESULTS

3.1 Influence of amplitude on unsteady aerodynamics

Unsteady C_l and C_m for each heaving and pitching amplitude are shown in Figure 3. Magnitude of unsteady aerodynamics is normalized by the amplitude of forced oscillation, therefore the magnitude and also phase would be constant to any amplitude if it is linear.

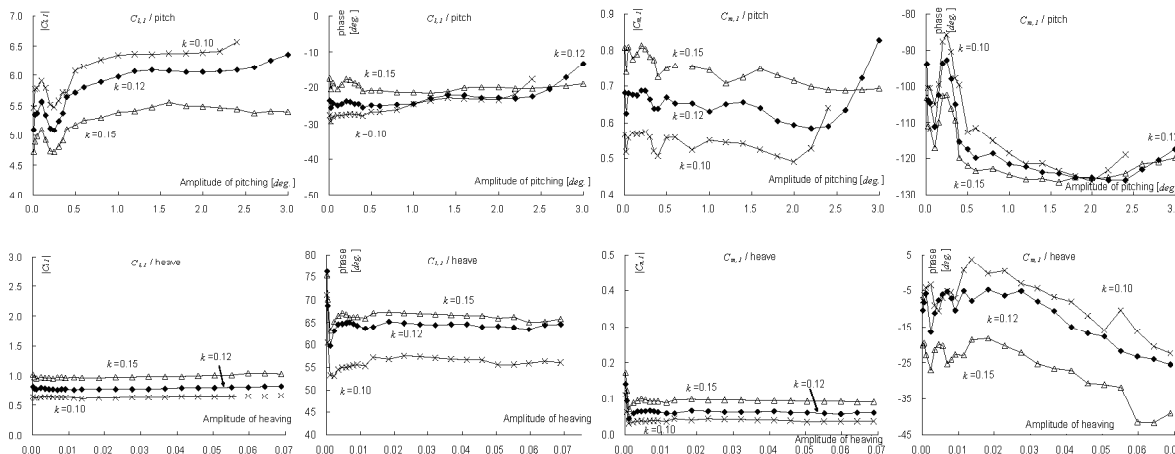


Figure 3 : Unsteady C_l and C_m for heaving and pitching mode

Figure 3 shows variation of the unsteady aerodynamics with smaller than amplitude 0.5 deg. , besides the large amplitude. In the calculation of pitching oscillation with $k=0.10$, those were not converged over amplitude 2.4 deg.

3.2 Influence of unsteady aerodynamics variation on stability boundary caused by amplitude

Stability boundary obtained by the $p-k$ analysis with superposed aerodynamics is shown in Figure 4.

Flutter index F_i is $F_i = 1 / \omega_\alpha * \sqrt{\mu} = (U / b \omega_\alpha) / \sqrt{\mu}$. Variation of stability boundary can be seen like the unsteady aerodynamics. High stability region where flutter index is large appears over 2.5 deg. and also around 0.2 deg. in pitching amplitude.

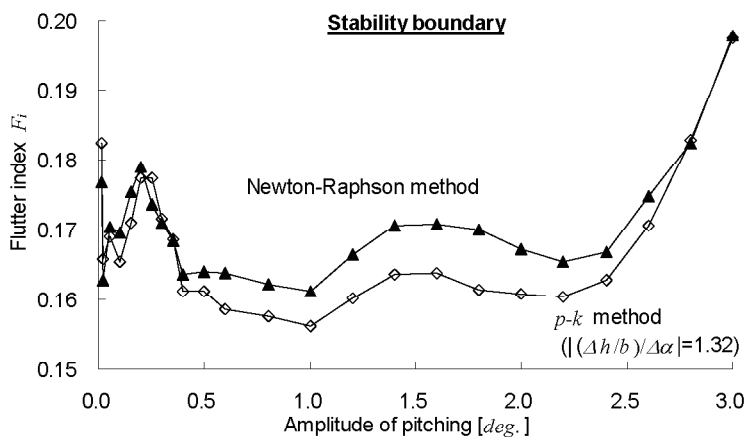


Figure 4 : Stability boundary

3.3 Evaluation of superposing unsteady aerodynamics

In transonic regime, linear stability analysis such as $U-g$ method, $p-k$ method, etc. can be more accurate using unsteady aerodynamics computed by transonic code. If unsteady aerodynamics is computed for each mode and those are superposed for the stability analysis, only infinitesimal small

amplitude is exact solution. Superposing effect is investigated and it is shown in Figure 5. Unsteady aerodynamics for the heaving and pitching mode which is $h/\alpha=1.32$, phase lag $\angle(h-\alpha)=10deg.$ and $k=0.12.$ are calculated. Triangle marks are unsteady aerodynamics directly obtained by the mode and circles are obtained by superposing two unsteady aerodynamics separately computed for heaving and pitching mode. Though the difference is small in smaller amplitude than $0.5deg.$, there is a certain difference in larger amplitude than that.

Stability boundary obtained by Newton-Raphson method is shown in Figure 4. It shows higher stability than $p-k$ method between 0.5 and $2.5deg.$ of pitching amplitude. Although the difference of flutter index is 5% at maximum, the shape of the boundary looks similar.

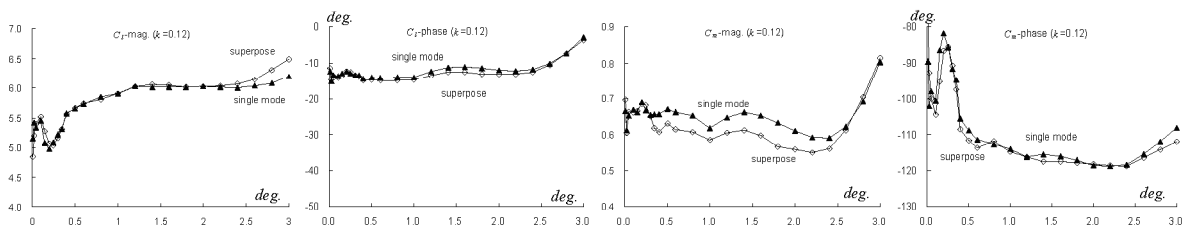


Figure 5 : Superposing effect (Unsteady C_l and C_m for pitching mode)

3.4 LCO amplitude related to the stability boundary

In Figure 4, stability boundary is shown and above the boundary the system is unstable and below the line it is stable. Oscillation diverges with the condition above the boundary and converges below the boundary. On a part of the line where it has plus inclination, oscillations come to the point on the line at a constant F_i , which is stable equilibrium. Exchanging x and y axis, it looks familiar bifurcation diagram.

At $F_i=0.175$, two stable equilibria exist at pitching amplitude 0.13 and $2.6 deg.$ Simulation starting with large initial value which is velocity corresponding to the one $deg.$ pitching amplitude results in the LCO with pitching amplitude $2.6 deg.$ (Figure 6 right). With smaller initial value, resulting LCO amplitude is about $0.9 deg.$ (Figure 6 left). The bifurcation diagram is confirmed by LCO simulations. Phase graph in LCO oscillation is shown in Figure 7. Higher harmonic component is

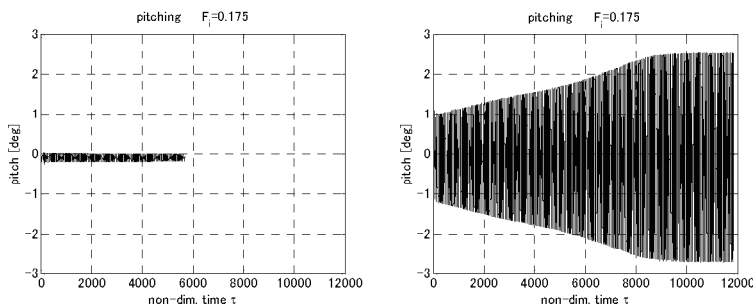


Figure 6 : LCO simulation

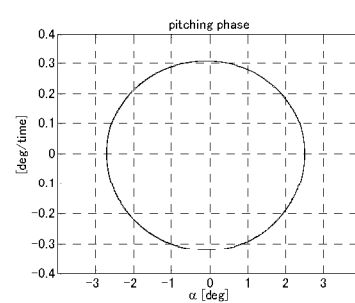


Figure 7 : Phase graph on LCO

small and taking first harmonic component of unsteady aerodynamics seems to be valid.

3.5 Considering nonlinearity in small amplitude oscillation

Variation of unsteady aerodynamics and stability boundary in small amplitude of oscillation has been observed by numerical analysis. In this section, we see what is happening in that region.

More than 2 deg. of pitching amplitude breaks the sinusoidal motion of the shock wave. Though shock wave propagates upstream as pitch goes up, the shock does not come back downstream and new shock appears after pitch goes down. Massive flow separation is generated and BL turbulence model may not calculate correctly.

On the other hand in less than amplitude 0.5 deg., peak of the unsteady pressure distribution can be observed around 0.2c besides around 0.65c. This wing profile shows that as the incidence decreases the pressure sinks at the center of the supersonic region on the upper surface, at which the peak appears in unsteady pressure distribution.

To see what is happening to the unsteady aerodynamics with small amplitude oscillation, effect of the transition point was investigated. In all of the calculations described above, transition points are automatically obtained, where turbulence viscosity coefficients μ_{tur} become 14. In this case the transition point is about 18%c. In Figure 9, unsteady pressure distributions and unsteady C_l are shown with the transition points automatically calculated, fixed at leading edge and 18%c. The peak of the unsteady pressure distribution moves upstream with the leading edge transition. Variation of the unsteady C_l becomes small with leading edge transition in small amplitude (Figure 8). So it can be said that the small amplitude LCO is affected by transition point or Reynolds number.

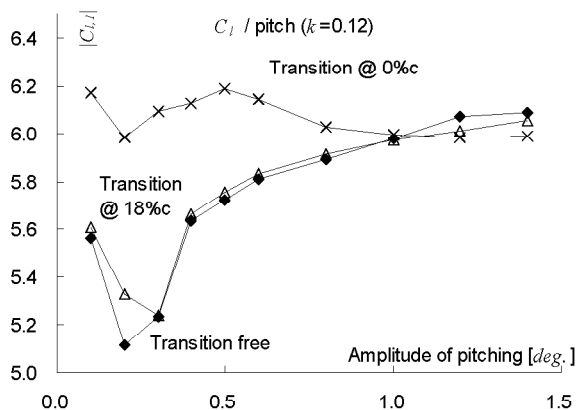


Figure 8 : Transition effect on unsteady C_l

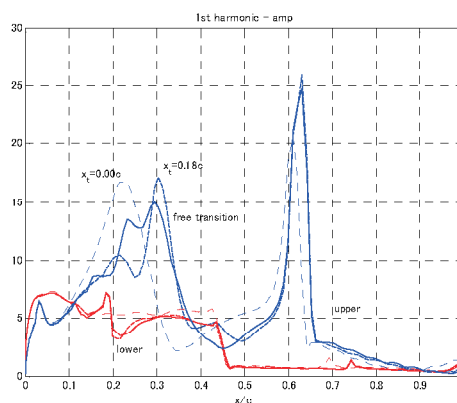


Figure 9 : Transition effect on Unsteady C_p distribution

4. CONCLUSION

NS analysis with free transition shows variation of unsteady aerodynamics in small amplitude range that is smaller than 0.5 *deg.* in pitching oscillation. This also affects stability boundary. Nonlinear phenomena such as LCO can be estimated by stability analysis with linear approximation. The *p-k* method with superposed unsteady aerodynamic coefficients can also specify the stability boundary, although it has a little error, in this case it is 5% of flutter index. Small amplitude LCO had been observed in the experiment might be the effect of transition point near the center of the supersonic region on the upper surface of the supercritical wing. If it can be confirmed by the experiment, supercritical wing with natural laminar flow might be exposed to small amplitude oscillation.

5. REFERENCES

- [1] G. Schewe, A. Knipfer, H. Mai, G. Dietz, "Experimental and Numerical Investigation of Nonlinear Effects in Transonic Flutter", DLR IB 232-2002J01
- [2] B. M. Castro, K. D. Jones, J. A. Ekaterinaris and M. F. Platzer, "Navier-Stokes Analysis of Wind-Tunnel Interference on Transonic Airfoil Flutter", AIAA Journal, Vol. 40, No. 7, July 2002, pp.1269-1276
- [3] J. P. Thomas, E. H. Dowell and K. C. Hall, "Modeling Viscous Transonic Limit-Cycle Oscillation Behavior Using a Harmonic Balance Approach", Journal of Aircraft, Vol. 41, No. 6, Nov.-Dec., 2004, pp.1266-1274
- [4] H. Kheirandish, G. Beppu and J. Nakamichi, "Numerical Flutter Simulation of a Binary System in Transonic Region", Aircraft Symposium, Hiroshima, Japan, 1995
- [5] R. J. Zwaan, "DATA SET 4, NLR 7301 Supercritical Airfoil Oscillatory Pitching and Oscillationg Flap", AGARD-R-702, 1982
- [6] U. R. Mueller, H. Henke, "Computation of Transonic Steady and Unsteady Flow about the NLR7301 Airfoil", Notes on Numerical Fluid Mechanics, Vol. 5x, pp.397-416, Commission of the European Communities, 1996